Available online at www.sciencedirect.com
ScienceDirect
Journal of Hazardous Materials 152 (2008) 1002–1010
Journal of Hazardous Materials
www.elsevier.com/locate/jhazmat

Thermal characteristics of aluminum nanoparticles and oilcloths

Yung-Chih Kuo [a,*], Hung-Kai Huang [a], Hong-Chun Wu [b]

[a] Department of Chemical Engineering, National Chung Cheng University, Chia-Yi 62102, Taiwan, ROC
[b] Institute of Occupational Safety and Health, Council of Labor Affairs, Taipei 221, Taiwan, ROC

Received 8 March 2007; received in revised form 23 July 2007; accepted 24 July 2007
Available online 28 July 2007

Abstract

Exothermic behavior of aluminum nanoparticles (ANP) in aqueous medium of various pH values and oilcloths (OC) composed of linseed oil, SAE 10W-40 engine oil, or SAE 20W-50 engine oil in cotton or nylon was studied. The experimental results revealed that for ANP hydrolysis, a deviation of pH value from 7 yielded a decrease in onset temperature (T_{onset}), peak temperature, no return temperature, self-accelerating decomposition temperature, time to T_{onset}, time to maximum rate (TMR_{ad}), and activation energy. Also, reaction order and frequency factor increased as pH value deviating from 7. For decomposition of oily materials, T_{onset} of OC was lower than that of pure oil, suggesting that cotton and nylon enhanced the combustibility of the three oils. Besides, total enthalpy of OC was larger than that of the corresponding pure oil. Nylon-based OC produced larger total enthalpy than cotton-based OC, while the latter yielded shorter oxidative induction time (OIT) than the former. Moreover, reasonable discrepancy between experimentally determined OIT and theoretically estimated TMR_{ad} was obtained. Hydrolysis of damped ANP and decomposition of OC could be derived from heat accumulation, leading to release of a considerable amount of thermal energy at relatively low T_{onset}.

Keywords: Thermal characteristics; Aluminum nanoparticle; Oilcloth; Time to maximum rate; Oxidative induction time

1. Introduction

Aluminum particles are one of the basic components of explosive and pyrotechnic materials. Also, aluminum powders were often utilized as painting extenders and coating pigments [1,2]. Combustion of aluminum nanoparticles, ANP, in air could be divided into two temperature stages: 1400 and 2800 K for a variety of products [3–5]. In humid conditions, water played a crucial role in exothermic ANP hydrolysis. The stoichiometry of ANP hydrolysis can be generally described by $xAl^{3+} + yH_2O \Leftrightarrow Al_x(OH)_y^{3x-y} + yH^+$, where x and y are two integers [6]. For the influence of water content, it was concluded that a high humidity in gas mixture of H_2O/O_2/Ar caused an advanced ignition of aluminum particles [7]. In systematic calorific heating of combustible substances, the temperature, at which the exothermic behavior begins, is defined as the onset temperature, T_{onset}. Note that T_{onset} is one of the most important properties of thermally hazardous materials. T_{onset} of ANP with average diameter of 10–100 nm decreased as the relative humidity increased [8]. Moreover, ANP could be still reactive over 47 days in surroundings with relative humidity of 90% [9,10]. Hence, self-heating in a system containing damped ANP might occur, leading to industrial accidents. For instance, serious explosion of Ju-Feng firecrackers and fireworks factory at Tunghsiao, Miaoli, Taiwan on 16 November 2003 was resulted from spontaneous combustion of damped aluminum particles during storage [11]. Furthermore, a relatively fast reaction of ANP hydrolysis was observed in an aqueous medium of a basic pH value [12]. The enthalpy of ANP hydrolysis in aqueous solution containing NaOH was very close to the heat of formation of $Al(OH)_4^-$ [13].

On the other hand, oilcloths, OC, composed of oils in fabrics, can be a kind of the spontaneously combustible materials because large specific surface area of absorbent results in heat

Abbreviations: ANP, aluminum nanoparticles; C80, Calvet 80 calorimeter; DSC, differential scanning calorimeter; OC, oilcloths

* Corresponding author. Tel.: +886 5 272 0411x33459; fax: +886 5 272 1206.
E-mail address: chmyck@ccu.edu.tw (Y.-C. Kuo).

0304-3894/$ – see front matter © 2007 Elsevier B.V. All rights reserved.
doi:10.1016/j.jhazmat.2007.07.075

Nomenclature

A	frequency factor (1/s)
C_p	heat capacity (J/g K)
D_{OC}	deviation between OIT_{OC} and $TMR_{ad,OC}$ (%)
D_{ANP}	deviation between OIT_{ANP} and $TMR_{ad,ANP}$ (%)
E	activation energy (kJ/mol)
n	reaction order
OIT	oxidative induction time (s)
P_{max}	maximum pressure (bar)
r	time ratio, $TMR_{ad,ANP}/t_{onset,ANP}$ or $TMR_{ad,OC}/t_{onset,OC}$
SADT	self-accelerating decomposition temperature (°C)
T_0	start temperature (°C)
T_{NR}	no return temperature (°C)
T_{onset}	onset temperature (°C)
T_p	peak temperature (°C)
T_S	surrounding temperature (°C)
TMR_{ad}	time to maximum rate under adiabatic condition (s)
ΔH	specific latent heat (J/g)
μ_{oil}	oil viscosity (Pa s)
ϕ	heating rate (°C/s)
ψ	rate of heat release (J/s g)
ψ_{onset}	rate of heat release corresponding to T_{onset} (J/s g)
$\psi(T_0)$	rate of heat release corresponding to T_0 (J/s g)

accumulation. Oils absorbed in cotton or sawdust may also belong to this category. Disused OC caused several conflagrations in supermarket warehouse and military depot [11]. For linseed oil-based OC, self-heating is initiated by gradual decomposition of unsaturated carbon bonds. Three oxidation stages of linseed oil, including oxidation of unsaturated fatty acids between 150 and 250 °C, first oxidative decomposition between 250 and 400 °C, and main process of combustion above 400 °C, were concluded [14]. In addition, the oxidation stability of oily substances can be assayed by iodine value and peroxide value [15,16]. For engine oils, thermal stability of SAE 15W-40 mixed with hydro-cracked oils was higher than that with refined oils [17]. Besides, oxidative induction time, OIT, defined as the time required for the initiation of oxidation under isothermal condition, was applied to the analysis of oxidation stability of lubricating oils [18]. Moreover, the degradation temperature of engine oils with larger viscosity was higher than that with smaller viscosity [19]. This suggested that engine oil with large viscosity would be thermally stable with large activation energy.

In poor ventilation system, heat accumulation is greater than heat dissipation by external heat source and/or self-heating of spontaneously combustible materials. For spontaneous combustion, thermal behavior can be analyzed by isothermal and temperature-programmed heating [20]. Differential scanning calorimeter, DSC, has been invoked to predict the coal combustibility [21] and the reactivity of self-reactive substances [22]. Also, self-accelerating decomposition temperature, SADT, of self-reactive substances has been evaluated by Calvet 80 calorimeter, C80 [23]. Hence, the two calorimetries could be appropriate for estimating the thermal properties of ANP and OC. In the present study, effect of pH value on the thermal characteristics of ANP hydrolyzed in aqueous medium was investigated. The exothermic system roughly mimicked the dampening situation during ANP storage in the case of contact with rainwater absorbing flare gases. Also, thermal decomposition of OC was examined. Linseed oil and the two commonly encountered engine oils, SAE 10W-40 and SAE 20W-50, were employed. In addition, fabrics were mostly made of cotton or nylon. Thus, combination of the three oils and the two fabrics simulated thermally hazardous OC in practice.

2. Materials and methods

2.1. Materials

ANP with average diameter of 18 nm were purchased from Junye (Shenzhen, Guangdong, China). Cotton of C-Yarn NE-20/1 and nylon of N-Yarn NE-19/1 were obtained from Formosa Chemicals & Fiber (Changhwa, Taiwan). Linseed oil with iodine value of 192 was purchased from MP Biomedicals (Irvine, California). SAE 10W-40 and SAE 20W-50 engine oils were obtained from FormulaShell (Houston, Texas). Hydroxyl chloride and sodium hydroxide were purchased, respectively, from Riedel-de Haën (Seelze, Germany) and Showa (Tokyo, Japan). Reverse osmosis purifier water was obtained from Waibel (Culligan-RO2127, Taoyuan, Taiwan).

2.2. Exothermic behavior examined by DSC and C80

ANP of approximate 3 mg was immersed in aqueous solution of 20 μL with various pH values. The ANP suspension was immediately placed in a high-pressure gold-plated steel crucible (ME-00026732, Mettler-Toledo, Greifensee, Switzerland) with diameter of 7 mm. DSC (Mettler DSC 822^e, Mettler-Toledo, Greifensee, Switzerland) at heating rate, ϕ, of 10 °C/min was employed to measure the exothermic properties. For the evaluation of kinetic parameters, DSC scanning at various ϕ values was applied. For the preparation of OC, oil (linseed oil, SAE 10W-40 engine oil, or SAE 20W-50 engine oil) of approximate 5 mg was absorbed by fabrics (cotton or nylon) of approximate 5 mg. Exothermic properties of the freshly fabricated OC were detected by DSC scanning in the gold-plated crucible at ϕ of 10 °C/min. For isothermal test, oil of approximate 60 mg was absorbed by fabrics of approximate 60 mg. OC was placed in a pressure detect vessel containing mix security crucible (S10/0057, Setaram, Caluire, France). C80 (Setaram-Calvet 80, Setaram, Caluire, France) was applied to investigate the exothermic trait. For the raise from room temperature to 200 °C, ϕ was fixed at 0.5 °C/min, and the C80 system was maintained at 200 °C. The isothermal duration was 24 h for cotton-based OC and 48 h for nylon-based OC.

2.3. Kinetic analysis

Activation energy of an exothermic chemical reaction, E, can estimated by [24]

$$\ln\left(\frac{\phi}{T_p^2}\right) = C_K - \frac{E}{R}\frac{1}{T_P}, \tag{1}$$

$$\log\phi = C_O - 0.4567\frac{E}{R}\frac{1}{T_P}, \tag{2}$$

where T_p is the peak temperature in DSC thermogram, C_K and C_O are, respectively, the constants in the formula of Kissinger [25] and Ozawa [26], and R is the ideal gas constant. Besides, frequency factor, A, can be evaluated by [27]

$$A = \frac{\phi E\, e^{E/RT_p}}{RT_p^2}. \tag{3}$$

Based on the Freeman–Carroll's approach equation [28,29], reaction order, n, can be obtained:

$$n = \frac{\log[(dH/dt)_3/(dH/dt)_1]/(1/T_1 - 1/T_3) - \log[(dH/dt)_2/(dH/dt)_1]/(1/T_1 - 1/T_2)}{\log(\Delta H_1/\Delta H_2)/(1/T_1 - 1/T_2) - \log(\Delta H_1/\Delta H_3)/(1/T_1 - 1/T_3)}$$
$$= \frac{((1/T_1) - (1/T_2))\log[(dH/dt)_3/(dH/dt)_1] - ((1/T_1) - (1/T_3))\log[(dH/dt)_2/(dH/dt)_1]}{((1/T_1) - (1/T_2))\log(\Delta H_3/\Delta H_1) - ((1/T_1) - (1/T_3))\log(\Delta H_2/\Delta H_1)}, \tag{4}$$

where T_i, $(dH/dt)_i$, and ΔH_i, $i = 1, 2$, or 3, stand for the exothermic temperature, the rate of enthalpy change at T_i and the enthalpy change at T_i, respectively. These parameters were exemplified in Fig. 1, a typical DSC scanning thermogram of ANP. Moreover, time to maximum rate under adiabatic condition, TMR_{ad}, can be calculated by [30–32]

$$TMR_{ad} = \frac{C_p RT_0^2}{\psi(T_0)E}, \tag{5}$$

$$\psi(T_0) = \psi_{onset}\exp\left[\frac{E}{R}\left(\frac{1}{T_{onset}} - \frac{1}{T_0}\right)\right], \tag{5a}$$

where C_p represents the heat capacity, T_0 means the start temperature, $\psi(T_0)$ and ψ_{onset} denote the rate of heat release at T_0 and T_{onset}, respectively. C_p of ANP is 897.0 at 298.15 K, 930.6 at 350 K, and 955.5 at 400 K [33]. C_p of linseed oil, SAE 10W-40 engine oil, and SAE 20W-50 engine are, respectively, 448.5, 619.1, and 664.3 J/kg K [34]. Fig. 1 also demonstrated the relevant parameters appeared in Eqs. (5) and (5a). In addition, the discrepancy between TMR_{ad} and OIT can be expressed by

$$D_j = \frac{TMR_{ad,j} - OIT_j}{OIT_j} \times 100\%, \quad j = \text{ANP or OC}, \tag{6}$$

Furthermore, no return temperature, T_{NR}, is the temperature when rate of heat accumulation, Q_A, equal to rate of heat loss, Q_L. Hence, T_{NR} can be calculated by [22]

$$Q_A = \Delta HA\exp\left(-\frac{E}{RT_{NR}}\right) = Q_L = US(T_{NR} - T_S), \tag{7}$$

where ΔH, U, S, and T_S are, respectively, the overall enthalpy change, the overall heat transfer coefficient, the exposed surface area of materials, and the surrounding temperature. Note that U of ANP, linseed oil, SAE 10W-40 engine oil, and SAE 20W-50 engine are, respectively, 220, 130, 116, and 108 W/m^{2}K [34]. If T_S is greater than T_{NR}, exothermic reaction occurs. On the contrary, if T_S is smaller than T_{NR}, exothermic reaction may not certainly occur. Also, SADT is equivalent to T_S when reaction occurred within 7 days of storage and/or transportation, and can be formulated by [23,35]

$$SADT = T_S = T_{NR} - \left(\frac{RT_{NR}^2}{E}\right), \tag{8}$$

Substituting Eqs. (8) into (7) yields:

$$\Delta HA\exp\left(-\frac{E}{RT_{NR}}\right) = US\left(\frac{RT_{NR}^2}{E}\right). \tag{9}$$

T_{NR} can be determined by Eq. (9). Substituting the resultant T_{NR} into Eq. (8), SADT can be obtained.

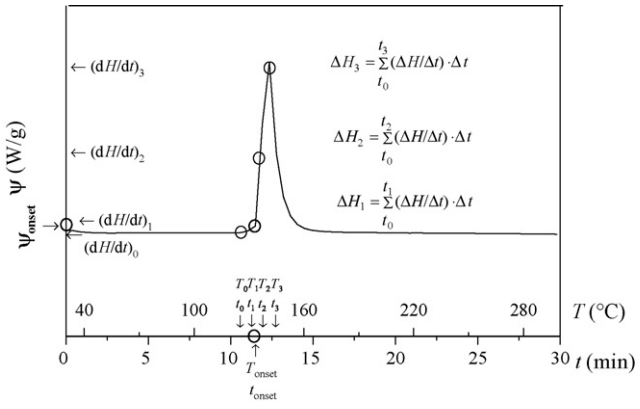

Fig. 1. Typical DSC thermogram of aluminum nanoparticles in aqueous solution: variation in rate of heat flow, ψ, as a function of temperature, T, and time, t. pH 7 and heating rate, $\phi = 10\,^\circ$C/min.

3. Results and discussion

3.1. Effect of pH value on the thermal properties of ANP

Table 1 lists the variations in T_{onset}, T_p, ΔH, and n as a function of pH value for ANP. As shown in Table 1, the highest T_{onset} and T_p and the smallest n occurred at pH 7. Note that T_{onset} stood for the liability of the exothermic reaction. Also, the greater the deviation of pH value from 7, the lower T_{onset} and T_p and the larger n. The order of T_{onset} followed pH 13 < pH 1 < pH 11 < pH 3 < pH 9 < pH 5 < pH 7, indicating that the exothermic reaction of ANP could be accelerated by acidic or basic ingredients. The range of T_{onset} obtained by the present DSC scanning

Table 1
Thermal properties and reaction order of aluminum nanoparticles

pH	T_{onset} (°C)	T_p (°C)	ΔH (J/g)	n
1	93.59	114.10	4760.20	2.5285
3	139.32	154.17	4901.38	2.3012
5	140.87	154.89	5298.78	1.9725
7	141.33	156.41	5490.46	1.8666
9	140.12	153.99	5210.63	1.8979
11	135.25	148.89	4970.46	2.4309
13	79.85	92.65	6104.52	2.7932

was consistent with the study of ANP in aqueous solution by an adiabatic reaction calorimeter [9,10]. For oxidation of desiccated ANP in air, T_{onset} was located in 400–500 °C [9]. It has also been observed that the enthalpy of damped ANP was much higher than that of desiccated ANP [10]. In the present study, the largest and smallest ΔH occurred at pH 13 and 1, respectively. This was mainly because in extremely strong basic medium, a large amount of complex compounds such as $Al(OH)_4^-$ was produced [36]. On the contrary, medium at pH 11 might inhibit exothermic process of ANP although pH 11 was a commonly recognized strong basic condition. Hence, ΔH at pH 11 exhibited the smallest enthalpy among the basic mediums. Complex compounds including $Al_{13}O_4(OH)_{24}(H_2O)_{12}^{7+}$ was formed in neutral to weak acidic medium, $Al(OH)_2^+$, $Al_2(OH)_2^{4+}$, and $Al_3(OH)_2^{7+}$ were produced in acidic medium, and Al^{3+} was the key products in strong acidic medium [36,37]. For simplicity, the stoichiometry of the reactions in aqueous medium of various pH values was briefly summarized below.

$2Al + 6H_2O + 2NaOH \rightarrow 2Na^+ + 2Al(OH)_4^- + 3H_2\uparrow$ with $-r_{Al} = kC_{Al}{}^2C_{H_2O}{}^6C_{NaOH}{}^2$ in base [12], $2Al + 6H_2O \rightarrow 2Al(OH)_3\downarrow + 3H_2\uparrow$ with $-r_{Al} = kC_{Al}{}^2C_{H_2O}{}^6$ in neutral water [6], and $2Al + 3H_2O + 3HCl \rightarrow AlCl_3\downarrow + Al(OH)_3\downarrow + 3H_2\uparrow$ with $-r_{Al} = kC_{Al}{}^2C_{H_2O}{}^3C_{HCl}{}^3$ in acid [38]. In these expressions, $-r_{Al}$ and k denoted the reaction rate of ANP and the rate constant, respectively. In the present DSC thermograms, the rate of heat flow increased rapidly to a maximum and then decreased rapidly. This feature corresponded to an nth order reaction [22]. Based on the rate equations described above, the reaction rate was almost proportional to the square of ANP concentration, which was consistent with the n values shown in Table 1. Furthermore, a greater deviation of pH from 7 caused a larger increase in the rate of heat flow during exothermic reaction. The numerical calculation revealed that the order of variation in the rate of heat flow affected by pH was $(dH/dt)_3 > (dH/dt)_2 > (dH/dt)_1$. Hence, a greater deviation of pH from 7 yielded a larger numerator of Eq. (4) and a larger n value. Generally, T_{onset}, T_p and ΔH in basic medium were lower than those in acidic medium under the same deviation from pH 7. On the contrary, under the same concentration of OH^- or H^+, n in OH^--rich medium were larger than that in H^+-rich medium. The main rationale behind this asymmetric behavior is that the reactivity of OH^- and ANP is higher than that of H^+ and ANP.

3.2. Kinetic parameters of ANP hydrolysis

Fig. 2 shows the plots for the evaluation of E based on Eqs. (1) and (2) at various ϕ values. The results of T_{onset}, T_p, E, A, T_{NR}, and SADT were listed in Table 2. As presented in this table, a lower ϕ led to lower T_{onset} and T_p. This was because to reach a specified temperature, a lower ϕ required a longer heating period and released a larger thermal energy. Furthermore, the order of pH value on A was pH 13 > pH 1 > pH 7. An increased A value in acidic and basic medium could be resulted from an increased collision frequency between ANP and H^+ or OH^-. The reverse order of pH value was true for E, T_{NR}, and SADT. These results implied that an exothermic effect of ANP was most susceptible to a medium of strong base. Moreover, E and A estimated by the Kissinger's method were slightly larger than those by the Ozawa's. Hence, T_{NR} and SADT estimated by the Kissinger's method were slightly smaller than those by the Ozawa's, as indicated in Table 2. However, these parameters evaluated by the both methods were on the same order of magnitude.

Table 2
Kinetic parameters of aluminum nanoparticles

pH	ϕ (°C/min)	T_{onset} (°C)	T_p (°C)	Kissinger's method		Ozawa's method		T_{NR} (°C)		SADT (°C)	
				E (kJ/mol)	A (1/s)	E (kJ/mol)	A (1/s)	$T_{NR,K}$[a]	$T_{NR,O}$[b]	$SADT_K$[a]	$SADT_O$[b]
1	2	53.45	80.33	24.868	6.05×10^{15}	24.568	4.08×10^{15}	58.98	60.77	22.134	23.078
	4	74.86	94.95								
	8	90.01	108.91								
	10	93.59	114.10								
7	2	117.00	126.23	71.211	2.62×10^{10}	70.989	2.45×10^{10}	66.96	70.32	53.467	56.516
	4	126.12	137.09								
	8	138.69	152.31								
	10	141.33	156.41								
13	2	59.41	65.55	23.511	1.52×10^{18}	23.461	1.40×10^{18}	49.85	50.06	12.991	13.045
	4	68.66	76.70								
	8	74.63	84.20								
	10	79.85	92.65								

[a] Subscript K denotes data estimated by the Kissinger's method.
[b] Subscript O denotes data estimated by the Ozawa's method.

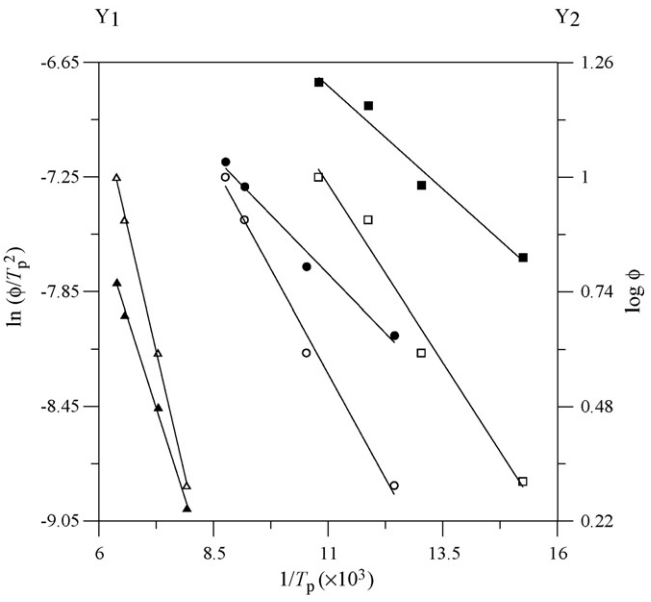

Fig. 2. Plots for the methods of Kissinger and Ozawa. ▲, ● and ■: the Kissinger's method using Y_1 axis; △, ◯, and □: the Ozawa's method using Y_2 axis. ▲ and △ for pH 1, ● and ◯ for pH 7, ■ and □ for pH 13. ▲: $R = 0.9915$, ●: $R = 0.9984$, ■: $R = 0.9857$, △: $R = 0.9956$, ◯: $R = 0.9992$, □: $R = 0.9881$.

Based on the present DSC scanning results, $TMR_{ad,ANP}$ calculated by Eqs. (5) and (5a) was ca. 25.26 days at pH 7 and $T_0 = 25\,^{\circ}C$. From the data of isothermal ANP hydrolysis in neutral water [11], OIT_{ANP} and the predicted $TMR_{ad,ANP}$ were, respectively, ca. 560 and 689.9 min at $T_0 = 60\,^{\circ}C$, ca. 85 and 94.62 min at $T_0 = 80\,^{\circ}C$, and ca. 12 and 13.65 min at $T_0 = 100\,^{\circ}C$. Thus, D_{ANP} was 23.2% at $T_0 = 60\,^{\circ}C$, 11.3% at $T_0 = 80\,^{\circ}C$ at 13.75% $T_0 = 100\,^{\circ}C$. These results revealed that TMR_{ad} would be a reasonable prediction for the initiation of the exothermic hydrolysis of ANP under isothermal condition. Note that a shorter OIT denoted a lower thermal stability.

Fig. 3 presents the variation in $TMR_{ad,ANP}$, $t_{onset,ANP}$, and the ratio of the two, r, as functions of pH value. Here, $TMR_{ad,ANP}$ could be regarded as the upper limit of time to ANP hydrolysis. A large r represented a large discrepancy between adiabatic circumstance and programmed heating. As indicated in Fig. 3, the range of r was ca. 3–6. Also, an increase in deviation of pH value from 7 caused a decrease in $TMR_{ad,ANP}$, $t_{onset,ANP}$, and r, i.e., maxima occurred at pH 7. This implied that in acidic and basic medium, ANP became thermally instable and r value reduced. Thus, the relation between r and thermal stability suggested that r value could be a practical index for the assessment of thermally hazardous materials. Moreover, r was asymmetric when pH value deviated from 7. This was because the effect of OH^- on the reduction in r value was stronger than H^+. Based on the same $|pH-7|$, $t_{onset,ANP}$ in basic medium was shorter than that in acidic medium, implying that OH^- caused even faster exothermic reaction under adiabatic condition. In the current study, ln $TMR_{ad,ANP}$ and ln $t_{onset,ANP}$ were exhibited for a clear presentation. As pH value varied, ln $TMR_{ad,ANP}$ and ln $t_{onset,ANP}$ seemed to be symmetric. In fact, variations in the original time data as functions of pH value were not perfect symmetry. Logarithms of $TMR_{ad,ANP}$ and $t_{onset,ANP}$ eliminated the numerical asymmetry, yielding a pseudo-symmetric trait.

3.3. Thermal behavior of OC by DSC scanning

Fig. 4 exhibits the DSC thermograms of linseed oil, SAE 10W-40 engine oil, and SAE 20W-50 engine oil. As revealed in this figure, two exothermic peaks were emerged for the three oil species. This was consistent with the literature observation [14]. The first and second peaks might be the initiated interfa-

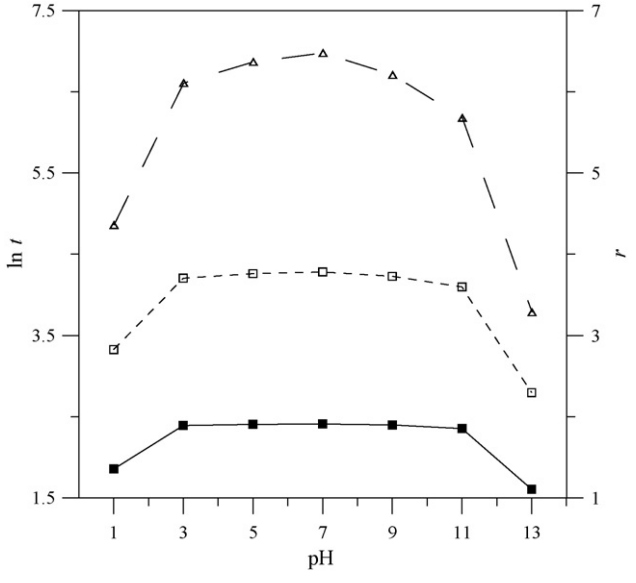

Fig. 3. Variation in logarithm of time, $\ln t$, and time ratio, $r = TMR_{ad,ANP}/t_{onset,ANP}$, as a function of pH value. t is $t_{onset,ANP}$, the time to T_{onset} obtained from dynamic DSC experiments of aluminum nanoparticles, or $TMR_{ad,ANP}$ based on T_{onset}. ■: $t_{onset,ANP}$; □: $TMR_{ad,ANP}$; △: r.

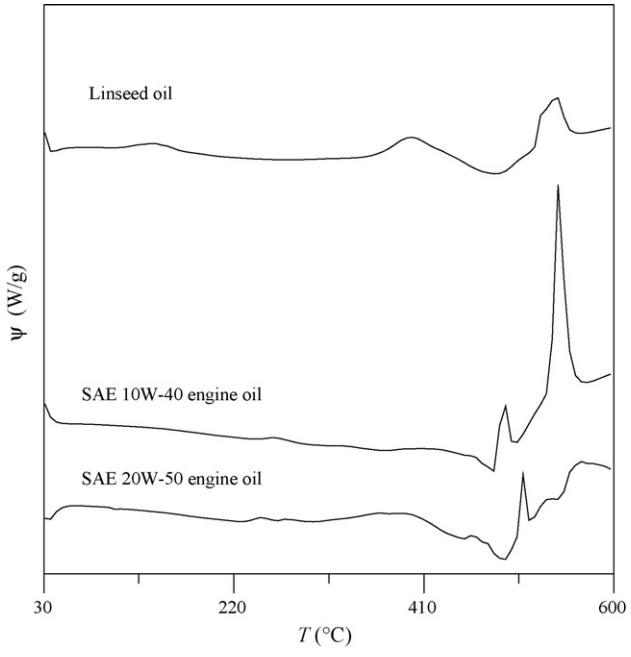

Fig. 4. DSC thermograms of linseed oil, SAE 10W-40 engine oil, and SAE 20W-50 engine oil.

cial oxidation and buck oxidation, respectively. Table 3 listed the exothermic characteristics of the oily materials by DSC scanning. For pure oil, the order of oil on T_{onset} and T_p was linseed oil < SAE 10W-40 engine oil < SAE 20W-50 engine oil, in general. $T_{onset,1}$ of OC followed the same order. These data suggested that linseed oil was prone to combustion, which was consistent with the literature results [18,19,39]. In addition, linseed oil belonged to combustible drying oil due to typical iodine value of 170–205 [15,16]. On the other hand, SAE 10W-40 was more liable to thermally decompose than SAE 20W-50. This was mainly because the former was less viscous the latter [26] and the former possessed lower activation energy than the latter [27]. For OC, the order of oil on $T_{onset,2}$, $T_{p,1}$, and $T_{p,2}$ became SAE 10W-40 engine oil < linseed oil < SAE 20W-50 engine oil, in general. As compared with pure oil, the alteration in the order was derived from the existence of fabric matrices. By the emergence of the polymeric materials, the bulk absorbability of 10W-40 engine oil might be higher than those of linseed oil. Thus, 10W-40 engine oil produced the lowest, $T_{onset,2}$, $T_{p,1}$, and $T_{p,2}$ among the three oil species, in general. It was also intriguing to note that for a fixed oil species, OC yielded an apparent decrease in T_{onset} and T_p of pure oil. This was because OC shortened the time to exothermic peaks by an increase in the exposed area and the peroxide value. Besides, our literature survey revealed that T_{onset} of linseed oil and linseed oil in cotton were, respectively, ca. 400 °C [14] and ca. 325 °C [39], which were close to the present results. It was also reported that by incorporation with linseed oil, the activation energy of pure cotton reduced in half [39]. Hence, requirement for combustion of OC was achieved more easily than that of pure oil. Moreover, during thermal treatment of oils, unsaturated carbon bonds were first decomposed, which was followed by an accelerated oxidative rate [40]. For linseed oil, $T_{onset,1}$ of cotton-based OC was lower than that of nylon-based OC. This was because the surface wettability of linseed oil on cotton was higher than that on nylon. Hence, cotton matrix was beneficial to the first-stage decomposition of linseed oil. On the contrary, for the two engine oils, $T_{onset,1}$ of cotton-based OC was higher than that of nylon-based OC. It could also be concluded that for a fixed oil species, the order on $T_{onset,2}$ was oil in nylon < oil in cotton < pure oil, in general. The rationale behind this result could be elaborated below. The decomposition temperatures of pure nylon and cotton were 220–280 °C [41,42] and 335–356 °C [43], respectively. Besides, T_{onset} of OC was between T_{onset} of pure fabric and that of oil. Since relatively viscous engine oils lowered the surface wettability on fabrics, decomposition temperature of pure fabrics became dominant on T_{onset} of OC. Thus, T_{onset} of engine oils in cotton was higher than that in nylon. For latent heat of pure oil and two oil-cloth composites, the order of oil on the total enthalpy was SAE 20W-50 engine oil < linseed oil < SAE 10W-40 engine oil. This result suggested that the various ingredients in SAE 10W-40 engine oil could release the highest thermal energy during combustion among the currently studied three oil species. On the contrary, the components of SAE 20W-50 engine oil generated the smallest capacity in enthalpy. For a fixed oil species, the order on ΔH_{total} was pure oil < oil in cotton < oil in nylon, implying that oil in nylon could be the most thermally hazardous materials among the three cases. Based on the enthalpy analysis, nylon containing SAE 10W-40 was the most potentially disastrous OC, if the accumulation heat led to the conditions of combustion.

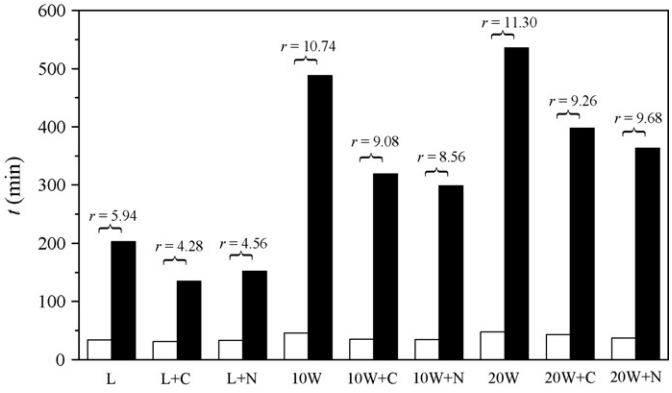

Fig. 5. Time, t, and time ratio, $r = TMR_{ad,OC}/t_{onset,OC}$, for various oils and oilcloths. t is $t_{onset,OC}$, the time to $T_{onset,1}$ obtained from dynamic DSC tests of oils and oilcloths, or $TMR_{ad,OC}$ based on $T_{onset,1}$. □: $t_{onset,OC}$, ■: $TMR_{ad,OC}$. L: linseed oil, L + C: linseed oil in cotton, L + N: linseed oil in nylon, 10W: 10W-40 engine oil, 10W + C: 10W-40 engine oil in cotton, 10W + N: 10W-40 engine oil in nylon, 20W: 20W-50 engine oil, 20W + C: 20W-50 engine oil in cotton, 20W + N: 20W-50 engine oil in nylon.

Fig. 5 shows $TMR_{ad,OC}$, $t_{onset,OC}$, and the ratio of the two, r, for various oily materials. As revealed in this figure, the theoretically predicted $TMR_{ad,OC}$ was longer than the experimentally obtained $t_{onset,OC}$. Hence, $TMR_{ad,OC}$ could be considered as the

Table 3
Thermal properties of oils and oilcloths

Oilcloths		$T_{onset,1}$ (°C)	$T_{p,1}$ (°C)	ΔH_1 (J/g)	$T_{onset,2}$ (°C)	$T_{p,2}$ (°C)	ΔH_2 (J/g)	ΔH_{total} (J/g)
Linseed oil	–	371.85	399.58	159.62	538.69	541.45	145.05	304.67
	Cotton	345.17	420.57	282.11	494.99	507.07	124.79	406.9
	Nylon	363.33	415.00	607.36	486.16	523.69	286.34	893.7
10W-40 engine oil	–	484.12	489.04	60.62	538.91	544.99	298.15	358.77
	Cotton	381.07	409.17	164.72	488.29	527.24	527.63	692.35
	Nylon	378.65	409.96	1132.07	452.65	468.68	99.99	1232.06
20W-50 engine oil	–	504.54	507.60	49.61	561.83	564.95	114.02	163.63
	Cotton	459.61	479.22	207.53	541.76	561.52	113.53	321.06
	Nylon	405.61	413.63	299.01	496.33	512.82	382.82	879.15

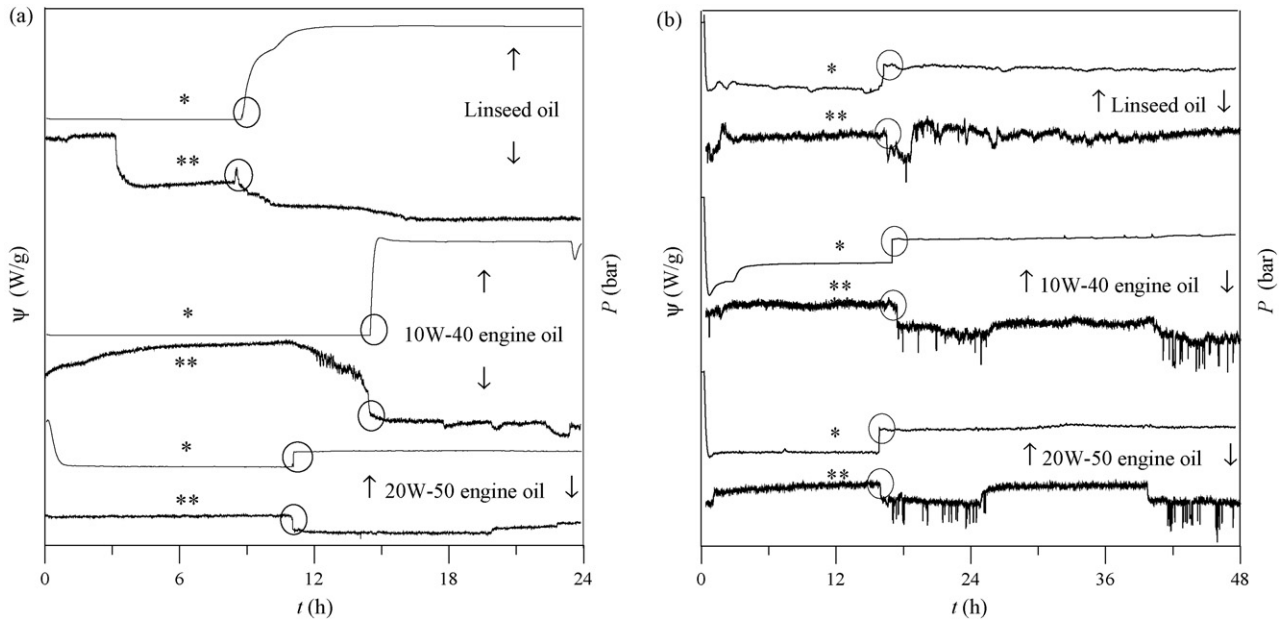

Fig. 6. C80 thermograms of oilcloths under isothermal temperature of 200 °C: variation in rate of heat flow, ψ, and pressure, P, as a function of time, t. * for ψ and ** for P. (a) Cotton-based oilcloths and (b) nylon-based oilcloths.

Table 4
Oxidative induction time, OIT_{OC}, and time to maximum rate, $TMR_{ad,OC}$, of oilcloths

Oilcloths		P_{max} (bar)	OIT_{OC} (min)	μ_{oil} (Pa s)	E (kJ/mol)	$TMR_{ad,OC}$ (min)	D_{OC} (%)
linseed oil	Cotton	3.95	480	–	79.2[b]	518	7.92
	Nylon	4.01	1032			1318	27.71
10W-40 engine oil	Cotton	4.07	828	0.04966[a]	95.25–103.2[c]	1072–1131	29.3–36.6
	Nylon	4.10	1056			1296–1419	22.7–34.4
20W-50 engine oil	Cotton	3.94	672	0.06548[a]	110.6–138.3[c]	708–756	5.36–12.5
	Nylon	3.98	1008			1202–1254	19.2–24.4

[a] Data from FormulaShell®.
[b] Data evaluated from Ref. [26].
[c] The range of data obtained via E–μ_{oil} relation in Ref. [27].

longest lag in the decomposition of OC. Besides, $TMR_{ad,OC}$ of pure oil was longer than that of OC. For a fixed oil species, r value of pure oil was also larger than that of OC, implying that oils became more combustible in fabrics. Moreover, r value of OC containing linseed oil was smaller than that of OC containing engine oils. This was consistent with the results of Table 3.

3.4. Isothermal decomposition of OC

Fig. 6(a) and (b) displays the thermograms of OC by C80 study. The resultant P_{max} and OIT_{OC} and the estimated $TMR_{ad,OC}$ at $T_0 = 200\,°C$ were summarized in Table 4. As shown in this table, P_{max} of the six OC during isothermal examination was close (ca. 4 bar), while SAE 10W-40 in nylon produced the largest P_{max}. Note that a higher P_{max} during combustion represented a more volatile OC, rendering a greater thermal effect. For a fixed oil species, OIT_{OC} of cotton-based OC was shorter than that of nylon-based OC. This was because OIT_{OC} was mainly determined by the oxidative area. A large area yielded a short OIT_{OC}. Since the density of cotton was less than nylon, at a fixed mass, the former possessed a larger exposed area for oil attachment than the latter. Moreover, the order of oil on OIT_{OC} for cotton-based OC was linseed oil < SAE 20W-50 engine oil < SAE 10W-40 engine oil. OIT_{OC} of the three nylon-based OC was ca. 1000 min. As compared with the estimated $TMR_{ad,OC}$, D_{OC} of approximate 10–30% was evaluated. Besides, D_{OC} of cotton-based OC was generally smaller than that of nylon-based OC.

4. Conclusions

Exothermic reaction of damped ANP could be accelerated in acidic or basic medium. From the analysis of T_{onset}, T_{peak}, ΔH, E, n, A, T_{NR}, and SADT, ANP in medium of pH 13 yielded the most prominent thermal effect. Besides, $TMR_{ad,ANP}$ was an efficient parameter for isothermal hydrolysis of ANP, and the predicted

$TMR_{ad,ANP}$ at pH 7 was ca 25 days. Also, a smaller ratio of $TMR_{ad,ANP}$ to t_{onset}, r, caused a faster hydrolysis of ANP. On the other hand, oils absorbed in fabrics lowered $t_{onset,1}$ because OC possessed a large oxidative area. As suggested by the results of $t_{onset,1}$ and OIT_{OC}, linseed oil in cotton was the most combustible OC among the six OC examined in the present study. Moreover, ΔH_{total} implied that nylon-based OC would potentially cause significant hazard. Especially, SAE 10W-40 in nylon yielded largest ΔH_{total} and P_{max} among the three nylon-based OC.

Acknowledgments

This work was supported by the National Science Council and Council of Labor Affairs of the Republic of China.

References

[1] P. Pelicon, M.K. Gunde, M. Kunaver, J. Simčič, M. Budnar, Analysis of metallic pigments by ion microbeam, Nucl. Instrum. Meth. Phys. Res. B 190 (2002) 370–374.
[2] M.M. Beppu, E.C.D.O. Lima, F. Galembeck, Aluminum phosphate particles containing closed pores: preparation, characterization, and use as a white pigment, J. Colloid Interface Sci. 178 (1996) 93–103.
[3] Y.S. Kwon, A.A. Gromov, A.P. Ilyin, G.H. Rim, Passivation process for superfine aluminum powders obtained by electrical explosion of wires, Appl. Surf. Sci. 211 (2003) 57–67.
[4] Y.S. Kwon, A.A. Gromov, A.P. Ilyin, E.M. Popenko, G.H. Rim, The mechanism of combustion of superfine aluminum powders, Combust. Flame 133 (2003) 385–391.
[5] A. Gromv, V. Vershchagin, Study of aluminum nitride formation by superfine aluminum powder combustion in air, J. Eur. Ceram. Soc. 24 (2004) 2879–2884.
[6] F. Roelofs, W. Vogelsberger, Dissolution kinetics of nanodispersed γ-alumina in aqueous solution at different pH: unusual kinetic size effect and formation of a new phase, J. Colloid Interface Sci. 303 (2006) 450–459.
[7] J. Servaites, H. Krier, J.C. Melcher, R.L. Buryon, Ignition and combustion of aluminum particles in shocked H_2O/O_2/Ar and CO_2/O_2/Ar mixtures, Combust. Flame 125 (2001) 1040–1054.
[8] Y. Li, W. Song, C.S. Xie, D. Zeng, A. Wang, M. Hu, Influence of humidity on the thermal behavior of aluminum nanopowders, Mater. Chem. Phys. 97 (2006) 127–131.
[9] Q.S.M. Kwok, R.C. Fouchard, A.M. Turcotte, P.D. Lightfoot, R. Bowes, D.E.G. Jones, Characterization of aluminum nanopowder compositions, Propell. Explos. Pyrot. 27 (2002) 229–240.
[10] D.E.G. Jones, R. Turcotte, R.C. Fouchard, Q.S.M. Kwok, A.M. Turcotte, Z. Abdel-Qader, Hazard characterization of aluminum nanopowder compositions, Propell. Explos. Pyrot. 28 (2003) 120–131.
[11] H.C. Wu, C.H. Huang, Y.C. Kuo, Identification of fire and explosion hazards of spontaneously combustible materials, J. Occup. Saf. Health 14 (2006) 308–319.
[12] R. Hellmann, The albite–water system. Part II. The time-evolution of the stoichiometry of dissolution as a function of pH at 100, 200, and 300 °C, Geochim. Cosmochim. Acta 59 (1995) 1669–1697.
[13] W.M. Zeng, Q.Y. Chen, X.M. Chen, Determination of the standard molar enthalpy of formation of the ion $Al(OH)_4^-$(aq), J. Chem. Thermodyn. 26 (1994) 205–210.
[14] M. Lazzari, O. Chiantore, Drying and oxidative degradation of linseed oil, Polym. Degrad. Stabil. 65 (1999) 303–313.
[15] C.J. Abraham, A solution to spontaneous combustion in linseed oil formulations, Polym. Degrad. Stabil. 54 (1996) 157–166.
[16] O.K. Guler, F.S. Guner, A.T. Erciyes, Some empirical equations for oxypolymerization of linseed oil, Prog. Org. Coat. 51 (2004) 365–371.
[17] J. Cerny, Z. Strnad, G. Sebor, Composition and oxidation stability of SAE 15W-40 engine oils, Tribol. Int. 34 (2001) 127–134.
[18] B.K. Sharma, A.J. Stipanovic, Development of a new oxidation stability test method for lubricating oils using high-pressure differential scanning calorimetry, Thermochim. Acta 402 (2003) 1–18.
[19] C.D. Gamlin, N.K. Dutta, M.R. Choudhury, D. Kehoe, J. Matisons, Evaluation of kinetic parameters of thermal and oxidative decomposition of base oils by conventional, isothermal and modulated TGA, and pressure DSC, Thermochim. Acta 392–393 (2002) 357–369.
[20] T. Ozawa, Thermal analysis review and prospect, Thermochim. Acta 355 (2000) 35–42.
[21] P. Garcia, P.J. Hall, F. Mondragon, The use of differential scanning calorimetry to identify coals susceptible to spontaneous combustion, Thermochim. Acta 336 (1999) 41–46.
[22] A. Miyake, M. Sumino, Y. Oka, T. Ogawa, Y. Iizuka, Prediction and evaluation of the reactivity of self-reactive substances using microcalorimetries, Thermochim. Acta 352–353 (2000) 181–188.
[23] Y. Yu, K. Hasegawa, Derivation of the self-accelerating decomposition temperature for self-reactive substances using isothermal calorimetry, J. Hazard. Mater. 45 (1996) 193–205.
[24] M. Malow, U. Krause, The overall activation energy of the exothermic reactions of thermally unstable materials, J. Loss. Prev. Process. Ind. 17 (2004) 51–58.
[25] H.E. Kissinger, Reaction kinetics in differential thermal analysis, Anal. Chem. 29 (1957) 1702–1706.
[26] T. Ozawa, Kinetic analysis of derivative curves in thermal analysis, J. Therm. Anal. 2 (1970) 301–324.
[27] M. Sunitha, C.P.R. Nair, K. Krishnan, K.N. Ninan, Kinetics of alderene reaction of tris(2-allylphenoxy)triphenoxycyclotriphazene and bismaleimides: a DSC study, Thermochim. Acta 374 (2001) 159–169.
[28] E.S. Freeman, B. Carroll, The thermogravimetric evaluation of the kinetics of the decomposition of calcium oxalate monohydrate, J. Phys. Chem. 62 (1958) 394–397.
[29] D.J. Peng, C.M. Chang, M. Chiu, Thermal reactive hazards of HMX with contaminants, J. Hazard. Mater. A114 (2004) 1–13.
[30] A. Keller, D. Stark, H. Fierz, E. Heinzle, K. Hungerbüher, Estimation of the time to maximum rate using dynamic DSC experiment, J. Loss. Prev. Process. Ind. 10 (1997) 31–41.
[31] G. Maria, E. Heinzle, Kinetic system identification by using short-cut techniques in early safety assessment of chemical processes, J. Loss. Prev. Process. Ind. 11 (1998) 187–206.
[32] J. Pastré, U. Wörsdörfer, A. Keller, K. Hungerbühler, Comparison of different methods for estimating TMRad from dynamic DSC measurements with ADT 24 values obtained from adiabatic Dewar experiments, J. Loss. Prev. Process. Ind. 13 (2000) 7–17.
[33] Y.C. Kuo, Study and identification of fires and explosions for the spontaneously combustible materials, Institute of Occupational Safety and Health, Taipei, 2006, pp. 55–56.
[34] J.D.J. Wales, L.M.L. Sanger, The Free Wikipedia Encyclopedia, 1st ed., Wikipedia, Houston, 2002.
[35] J. Sun, Y. Li, K. Hasegawa, A study of self-accelerating decomposition temperature (SADT) using reaction calorimetry, J. Loss. Prev. Process. Ind. 14 (2001) 331–336.
[36] M. Wang, M. Muhammed, Novel synthesis of Al_{13}-cluster based alumina materials, Nanostruct. Mater. 11 (1999) 1219–1229.
[37] E.A. El-Katatny, S.A. Halawy, M.A. Mohamed, M.I. Zaki, Surface composition, charge and texture of active alumina powders recovered from aluminum dross tailings chemical waste, Powder Technol. 132 (2003) 137–144.
[38] M.T. Swihart, L. Catoire, B. Legrand, I. Gokalp, C. Paillard, Rate constants for the homogeneous gas-phase Al/HCl combustion chemistry, Combust. Flame 132 (2003) 91–101.
[39] M.A. Khattab, A.A. El-Asael, S.H. Kandil, Effect of contamination of cotton fabric with linseed oil on the activation energies of pyrolysis and oxidation of the fabric, Fire Mater. 23 (1999) 131–137.

[40] Z.O. Oyman, W. Ming, R. van der Linde, Oxidation of drying oils containing non-conjugated and conjugated double bonds catalyzed by a cobalt catalyst, Prog. Org. Coat. 54 (2005) 198–204.

[41] H. Bockhorn, A. Hornung, U. Hornung, J. Weichmann, Kinetic study on the non-catalysed and catalysed degradation of polyamide 6 with isothermal and dynamic methods, Thermochim. Acta 337 (1999) 97–110.

[42] G.Z. Zhang, H. Yoshida, T. Kawai, Miscibility of Nylon 66 and Nylon 48 blend evaluated by crystallization dynamics, Thermochim. Acta 416 (2004) 79–85.

[43] L. Richard-Campisi, S. Bourbigot, M. le Bras, R. Delobel, Thermal behaviour of cotton-modacrylic fibre blends: kinetic study using the invariant kinetic parameters method, Thermochim. Acta 275 (1996) 37–49.